

Global Observation of Hydrogen/Deuterium Isotope Effects on Bidirectional Catalytic Electron Transport in an Enzyme: Direct Measurement by Protein-Film Voltammetry

Judy Hirst,[†] Brian A. C. Ackrell,[‡] and Fraser A. Armstrong^{*,†}

Contribution from the Inorganic Chemistry Laboratory, South Parks Road, Oxford, OX1 3QR, England, and VA Hospital and Department of Biochemistry and Biophysics, Molecular Biology Division, University of California, San Francisco, California 94121

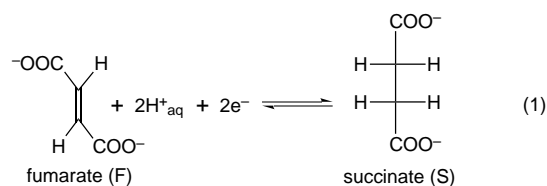
Received September 5, 1996[⊗]

Abstract: Protein-film voltammetry reveals the global effects of H/D isotopic substitutions, both in organic substrates and solvent, on bidirectional catalytic electron transport in a mitochondrial respiratory enzyme, succinate dehydrogenase. The voltammetry is controlled by the enzyme kinetics and therefore provides a direct display of the characteristic relationships between turnover rates (current) and driving force (potential). This enables simultaneous measurement of relative electron-transport rates for oxidative and reductive directions alongside thermodynamic data (reduction potentials) relating to substrates and active sites. Measured over a range of pH and pD, the relationships between effective catalytic potentials of the enzyme and formal reduction potentials for substrate and active-site yield a “potential-domain” description of the catalytic energetics, which complements and extends the picture obtained by conventional kinetic methods. For the organic substrates, a marked decrease is observed in the rate of oxidation of perdeuteriosuccinate compared to succinate, but there is no change upon deuterating fumarate. On changing the solvent from H₂O to D₂O there is a significant decrease in catalytic activity, particularly in the direction of fumarate reduction. Simultaneously, the characteristic potentials of the enzyme (active-site FAD and effective catalytic potentials) are raised but to a lesser extent than is the reduction potential of the substrate. The catalytic energetics are thus altered. For the first time with a complex redox enzyme, the results enable H/D substitution effects to be rationalized in terms of the changes introduced in overall driving force and enzyme reduction potentials, as well as the effects of intrinsic kinetic processes.

Introduction

Combining dynamic electrochemical techniques with H/D isotopic substitution is an attractive proposition for studying the processes which control the thermodynamics and kinetics of catalytic processes involving both proton and electron transfer in complex enzymes. Previously we used protein-film voltammetry^{1–6} to obtain direct measurements of the catalytic

performance of a respiratory-chain enzyme, succinate dehydrogenase, in response to variation in the electrochemical driving force.^{5,6} Succinate dehydrogenase (SDH), the membrane-extrinsic domain of mitochondrial Complex II⁷ contains a covalently bound FAD and three Fe–S clusters. The soluble enzyme adsorbs at a pyrolytic graphite edge (PGE) electrode from dilute (1 μM) solution, and displays bidirectional (i.e., oxidative and reductive) catalytic electron transport with (1:1) fumarate/succinate (F/S) mixtures in the contacting electrolyte, according to eq 1.^{5,6}



The voltammetry showed that neither interfacial electron transfer (the catalytic wave is reversible), substrate concentration ([S] = [F] ≫ K_M), nor mass transport of reactant (controlled by electrode rotation rate) is a rate limiting factor. This being the case, the relationships between rate and driving force thus revealed reflect kinetic barriers to electron transport *within* the enzyme–substrate complex. Accordingly, we have now examined the likelihood, and indeed confirmed, that the rates are controlled by various factors sensitive to H/D substitution.

(7) Ackrell, B. A. C.; Johnson, M. K.; Gunsalus, R. P.; Cecchini, G. In *Chemistry & Biochemistry of Flavoenzymes*; Müller, F., Ed.; CRC Press: Boca Raton, FL, 1992. Hederstedt, L.; Ohnishi, T. In *Molecular Mechanisms in Bioenergetics*; Ernster, L., Ed.; Elsevier: New York, 1992; pp 163–198.

[†] Inorganic Chemistry Laboratory.

[‡] University of California, San Francisco.

[⊗] Abstract published in *Advance ACS Abstracts*, July 15, 1997.

(1) Ideas of the scope of protein-film voltammetry are given in the following publications: (a) Armstrong, F. A. *Adv. Inorg. Chem.* **1992**, *38*, 117–163. (b) Armstrong, F. A.; Butt, J. N.; Sucheta, A. *Methods Enzymol.* **1993**, *227*, 479–500. (c) Armstrong, F. A. *Bioelectrochemistry of Biomacromolecules*. In *Bioelectrochemistry: Principles and Practice*, Vol. 5, Lenaz, G., Milazzo, G., Eds.; Birkhauser Verlag: Basel, 1997, Vol. 5, pp 205–255. (d) Armstrong, F. A.; Heering, H. A.; Hirst, J. *Chem. Soc. Rev.*, in press.

(2) Examples of endeavors to obtain structurally defined electroactive protein monolayers: Song, S.; Clark, R. A.; Bowden, E. F.; Tarlov, M. J. *J. Phys. Chem.* **1993**, *97*, 6564–6572. Feng, Z. Q.; Imabayashi, S.; Kakiuchi, T.; Niki, K. *J. Electroanal. Chem.* **1995**, *394*, 149–154.

(3) For examples of applications of protein-film voltammetry to study labile active sites, see: Butt, J. N.; Sucheta, A.; Martin, L. L.; Shen, B. H.; Burgess, B. K.; Armstrong, F. A. *J. Am. Chem. Soc.* **1993**, *115*, 12587–12588. Butt, J. N.; Niles, J.; Armstrong, F. A.; Breton, J.; Thomson, A. J. *Nat. Struct. Biol.* **1994**, *1*, 427–433. Duff, J. L. C.; Breton, J. L. J.; Butt, J. N.; Armstrong, F. A.; Thomson, A. J. *J. Am. Chem. Soc.* **1996**, *118*, 8593–8603.

(4) Sucheta, A.; Cammack, R.; Weiner, J.; Armstrong, F. A. *Biochemistry* **1993**, *32*, 5455–5465. Mondal, M. S.; Fuller, H. A.; Armstrong, F. A. *J. Am. Chem. Soc.* **1996**, *118*, 263–264.

(5) Sucheta, A.; Ackrell, B. A. C.; Cochran, B.; Armstrong, F. A. *Nature* **1992**, *356*, 361–362. Ackrell, B. A. C.; Armstrong, F. A.; Cochran, B.; Sucheta, A.; Yu, T. *FEBS Lett.* **1993**, *326*, 92–94.

(6) Hirst, J.; Sucheta, A.; Ackrell, B. A. C.; Armstrong, F. A. *J. Am. Chem. Soc.* **1996**, *118*, 5031–5038.

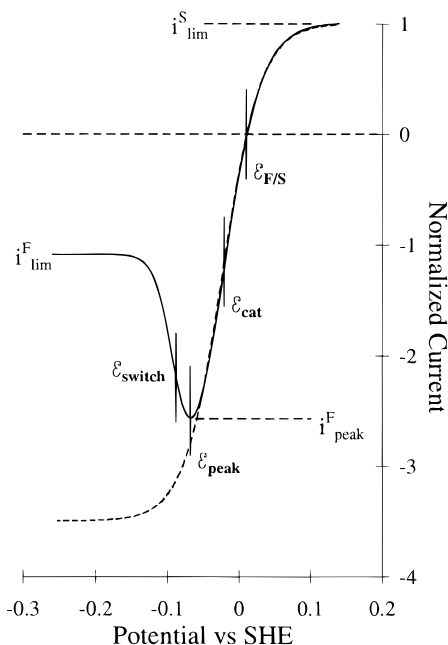


Figure 1. An idealized difference voltammogram or catalytic profile for SDH acting on a 1:1 succinate/fumarate mixture (pH 7.0, 38 °C) showing the i - E characteristics used to map out the kinetic and thermodynamic effects of exchanging H for D. The experimentally measured parameters $i_{\text{lim}}^{\text{S}}$, $i_{\text{peak}}^{\text{F}}$, and $i_{\text{lim}}^{\text{F}}$ reflect rates of succinate oxidation and fumarate reduction by the more active (high potential) and less active (low potential) forms of the enzyme respectively. $E_{\text{F/S}}$ is the isobestic potential (and Nernstian potential of the substrates) and E_{peak} is the potential of maximum fumarate reduction activity. The other two parameters are derived from simulation: E_{switch} is the potential of the site effecting transition between the more and less active forms, assigned as the FAD potential, while E_{cat} is the “catalytic” potential of the enzyme, i.e., the half height potential of the more-active-form catalytic wave [shown completed, in the absence of transition to the less-active form by (-)].

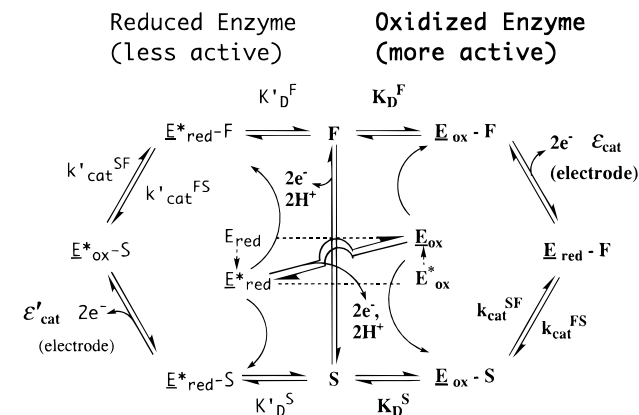
Electron transport in enzymes may be limited by proton-transfer restrictions to a far greater extent than is widely believed.^{8,9}

Kinetic isotope (H/D effects) are a well-established way of tracing rate-determining H atom transfer processes.¹⁰ However, to date, there have been few studies of kinetic isotope effects on electron-transport enzymes.^{11–13} Moreover, there is little knowledge of the extent to which H/D substitutions alter the reduction potentials of active sites and substrates, and thus influence the rates by changing the driving force and catalytic energetics.¹¹ By using protein-film voltammetry it is possible to measure and deconvolute the complex effects of H/D substitution on the entire catalytic process, i.e. the rates of reaction in each direction and, simultaneously, the underlying thermodynamics. Effects due to intrinsic changes in rates of the chemical reaction are therefore viewed alongside changes

(8) Catalytic electron transport in bacterial photoreaction centers is limited by the rate of proton transfer to a buried quinone group. Away from conductive water channels, proton transfers are restricted (see ref 9) by the proximity of suitable bases. See: Okamura, M. Y.; Feher, G. *Annu. Rev. Biochem.* **1992**, *61*, 861–896. Takahashi, E.; Wraight, C. A. *Biochemistry* **1992**, *31*, 855–866.

(9) The much lower tunneling capability of hydrogen nuclei compared to electrons is an interesting concept, having obvious relevance to complex electron-transport enzymes and is described in articles by Klinman. A convenient comparison uses the de Broglie wavelengths of the two species, that of the electron being approximately 43 times greater than that of the proton, reflecting its much higher ability to tunnel through energy barriers and over larger distances. See for example: Klinman, J. P. *Trends Biochem. Sci.* **1989**, *14*, 368–377. Rucker, J.; Cha, Y.; Jonsson, T.; Grant, K. L.; Klinman, J. P. *Biochemistry* **1992**, *31*, 11489–11499. Bahnson, B. J.; Park, D.-H.; Kim, K.; Plapp, B. V.; Klinman, J. P. *Biochemistry* **1993**, *32*, 5503–5507. Jonsson, T.; Edmondson, D. E.; Klinman, J. P. *Biochemistry* **1994**, *33*, 14871–14878. Bahnson, B. J.; Klinman, J. P. *Methods Enzymol.* **1995**, *249*, 373–397.

Scheme 1



in driving force governing the enzyme’s catalytic ability, such as alterations in the reduction potentials of redox centers.

Previously we exploited the “binary” (all-or-nothing) decay of the voltammetric activity to produce a difference-voltammogram—the catalytic profile of the enzyme—by subtraction of successive cycles (thus removing non-Faradaic background current). Such a profile is shown in Figure 1. At high potential, succinate oxidation reaches a limiting rate represented by $i_{\text{lim}}^{\text{S}}$, but as the potential is lowered, fumarate reduction first reaches a maximum rate $i_{\text{peak}}^{\text{F}}$ before dropping to a lower constant level $i_{\text{lim}}^{\text{F}}$. This is a result of conversion to a less active form at a potential E_{switch} and is known as the “tunnel-diode” effect, due to similarity with the electronic device that displays *negative* resistance in a certain region of potential bias. The effect is linked to reduction of the FAD and may be considered in terms of the reduced FAD preferring an alternative conformation; thus, E_{switch} corresponds to the reduction potential of the FAD during turnover. The broken line in Figure 1 indicates the behavior which would be observed if such a conversion did not take place. The voltammetry can be modeled⁶ by taking into account further parameters also indicated in Figure 1 and shown in Scheme 1, i.e., E_{cat} (the catalytic or working potential of the enzyme), $E_{\text{F/S}}$ (the potential of the substrate couple), and E_{peak} (the potential of maximum fumarate reduction activity). A full explanation

(10) For general books and articles dealing with isotope effects, see, for example: Bell, R. P. *The Proton in Chemistry*, 2nd ed.; Chapman and Hall: London, 1973. Cleland, W. W. *Acc. Chem. Res.* **1975**, *8*, 145–151. More O’Ferrall, R. A. In *Proton Transfer Reactions*, Caldin, E. F., Gold, V., Eds.; Chapman and Hall: London, 1975. Albery, W. J. In *Proton Transfer Reactions*, Caldin, E. F., Gold, V., Eds.; Chapman and Hall: London, 1975. *Isotope Effects on Enzyme-Catalyzed Reactions*; Cleland, W. W., O’Leary, M. H., Northrop, D. B., Eds.; University Park Press: Baltimore, 1977. *Transition States of Biochemical Processes*, Gandour, R. D., Schowen, R. L., Eds.; Plenum Press: New York, 1978. Schowen, K. B.; Schowen, R. L. *Methods Enzymol.* **1982**, *87*, 551–606. *Enzyme Mechanism from Isotope Effects*; Cook, P. F., Ed.; CRC Press: Boca Raton, 1991.

(11) A kinetic study of H₂O/D₂O isotope effects on intramolecular ET in a multicenter flavoenzyme, xanthine oxidase, is described in: Hille, R. *Biochemistry* **1991**, *30*, 8522–8529.

(12) For further examples of H/D isotope effects on catalysis by complex ET enzymes, see: Batie, C. J.; Kamin, H. *J. Biol. Chem.* **1984**, *259*, 11976–11985. Beckmann, J. D.; Frerman, F. E. *Biochemistry* **1985**, *24*, 3922–3925. Okamura, M. Y.; Feher, G. *Proc. Natl. Acad. Sci. U.S.A.* **1986**, *83*, 8152–8156. D’Ardenne, S. C.; Edmondson, D. E. *Biochemistry* **1990**, *29*, 9046–9052. Döring, O.; Böttger, M. *Biochem. Biophys. Res. Commun.* **1992**, *182*, 870–876. Aikens, J.; Sliagar, S. G. *J. Am. Chem. Soc.* **1994**, *116*, 1143–1144. Bishop, G. R.; Davidson, V. L. *Biochemistry* **1995**, *34*, 12082–12086. Proshlyakov, D. A.; Ogura, T.; Shinzawa-Itoh, K.; Yoshikawa, S.; Kitagawa, T. *Biochemistry* **1996**, *35*, 8580–8586. Ogura, T.; Hirota, S.; Proshlyakov, D. A.; Shinzawa-Itoh, K.; Yoshikawa, S.; Kitagawa, T. *J. Am. Chem. Soc.* **1996**, *118*, 5443–5449.

(13) Studies of organic substrate isotope effects on catalysis by SDH are described in: Vitale, L.; Rittenberg, D. *Biochemistry* **1967**, *6*, 690–699. Hollocher, T. C.; You, K.; Conjalka, M. *J. Am. Chem. Soc.* **1970**, *92*, 1032–1035. Kaczorowski, G. J.; Cheung, Y.-F.; Walsh, C. *Biochemistry* **1977**, *16*, 2619–2628.

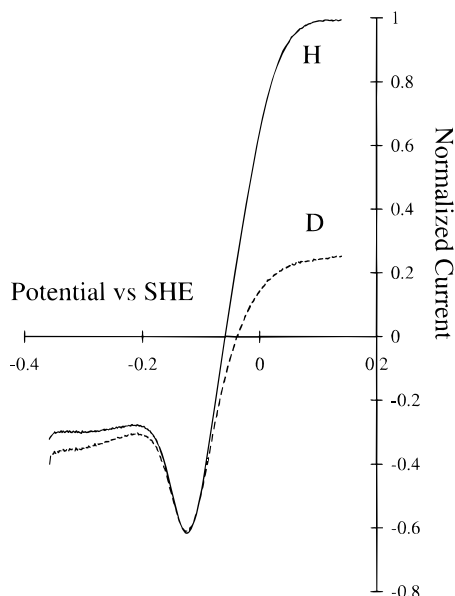


Figure 2. Comparison of difference voltammograms (typically subtraction of cycle 10 from cycle 2) obtained for H₂O solutions containing 5mM/5mM mixtures of F_H/S_H (—) and F_H/S_D (---). The currents are normalized to give equal $i_{\text{peak}}^{\text{F}}$ values. The PGE electrode was rotated at 400 rpm to optimize product dispersion. Temperature 38 °C, pH 7.8.

of the form of the voltammetry and of the modeling procedure is given in Appendix 1. A unique feature which voltammetric studies of this nature provide is the ability to quantify an electron-transport enzyme's intrinsic bias for preferring a particular direction of catalysis. This capability arises from the fact that one of the redox partners is the electrode which is able to provide a continuously variable driving force. As described in the Appendices, the catalytic bias is revealed from the separation between \mathcal{E}_{cat} and $\mathcal{E}_{\text{F/S}}$; this quantity relates to the ratio of limiting oxidation and reduction currents (ratio of rate constants), in this case as would be observed in the absence of the tunnel-diode effect. The example shown in Figure 1 is appropriate for pH 7.0, where the enzyme is seen to catalyze preferentially in the direction of fumarate reduction.

The data lead to an alternative perspective on catalytic electron transport, i.e., in the "potential domain", where characteristic features of the voltammogram serve as markers for active-site and substrate reduction potentials and, simultaneously, report on catalytic rates. We now describe how this methodology can be used to examine, at a glance, the interlinked kinetic and thermodynamic effects of solvent and substrate H/D (L) substitutions on a complex multicentered system.

Experimental Section

The procedures for isolating and handling SDH were as described previously.⁶ As before, all experiments were carried out in a glove box (Vacuum Atmospheres) under an N₂ atmosphere (O₂ < 2 ppm). Prior to experiments the enzyme samples were freed of residual ammonium sulfate, perchlorate, and most of the succinate by diafiltration (Amicon 8MC, YM30 membrane) against an appropriate (i.e., H₂O or D₂O) electrolyte solution. Supporting electrolyte consisted of 0.1 M NaCl (BDH) with a mixed buffer system of 10 mM HEPES [*N*-(2-hydroxyethyl)piperazine-*N'*-(2-ethanesulfonic acid)], 10 mM MES [2-(*N*-morpholino)ethanesulfonic acid], and 10 mM TAPS [*N*-[tris-(hydroxymethyl)methyl]-3-aminopropanesulfonic acid] all supplied by Sigma. Fumaric acid (99.5%) and succinic acid (99.5%) were supplied by Fluka, perdeuteriosuccinic acid (98%) was obtained from Aldrich, and perdeuteriofumaric acid (98.8%) was from Isotec Inc. The D₂O was of 99.9% purity. Following each experiment the pL (lyonium, L⁺ = H⁺, D⁺) of each cell solution was measured at the experimental (and physiological) temperature of 38 °C. Values of pL for D₂O

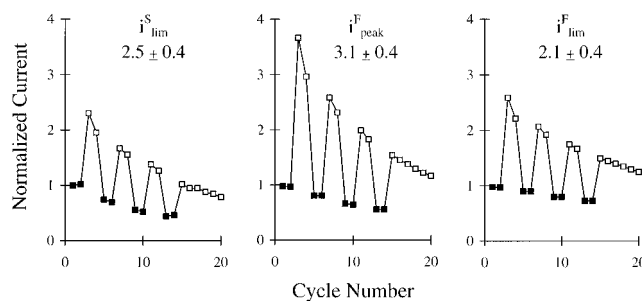


Figure 3. Currents obtained during a sequence of successive transfers between D₂O and H₂O solutions both containing 5mM/5mM F_H/S_H at pL = 7.4, temperature = 38 °C. Enzyme was adsorbed from the D₂O solution (■), two cycles were recorded, and the electrode was transferred (removing excess electrolyte) to the H₂O solution (□). Two cycles were recorded before returning to D₂O, and the procedure was continued. The results are presented relative to normalized first cycle currents measured in D₂O.

solutions were measured with a conventional glass electrode and corrected using the experimental relationship pD = meter reading + 0.40.¹⁴ No other assumptions or corrections were made. All voltammetry was carried out as described previously⁶ using an Autolab electrochemical analyzer (Eco-Chemie, Utrecht), except that experiments requiring rapid transfer of the enzyme between solutions utilized a "multipot" cell, which allows the separation of different cell solutions around a central reference electrode.^{1b}

Solutions with succinate (S) and fumarate (F) were made up by weight and concentrations were checked by enzymatic assay. For both S_H and S_D¹⁵ this was achieved by monitoring the SDH-catalyzed reduction of Fe(CN)₆³⁻ ($\epsilon_{420} = 1.03 \text{ mM}^{-1} \text{ cm}^{-1}$).⁷ For F_H and F_D, fumarase (EC 4.2.1.2, Sigma) was used to convert fumarate to L-malate. The oxidation of malate to oxalacetate [made irreversible by adduct formation with hydrazine (Aldrich, 98%)] was then coupled by malate dehydrogenase (EC 1.1.1.37, Fluka) to the reduction of β -NAD (Sigma) to NADH ($\epsilon_{340} = 6.22 \text{ mM}^{-1} \text{ cm}^{-1}$) at 35 °C.¹⁶

Results and Discussion

(1) Voltammetric Observation of Substrate Isotope Effects. Figure 2 shows the effect on the SDH catalytic profile of exchanging succinate for perdeuteriosuccinate (i.e., S_H for S_D), by comparing the difference voltammograms obtained with equal concentration mixtures of F_H/S_H and F_H/S_D.¹⁵ The voltammograms (only oxidative scans are shown for simplicity) have the characteristic form reported previously^{5,6} and the marked decrease in succinate oxidation rate ($i_{\text{lim}}^{\text{S}}$) on deuteration (effective isotope effects of 4.5 ± 0.5 at pH 7.4 and 3.5 ± 0.5 at pH 7.8) corresponds with that anticipated from classical experiments¹³ in which isotope effects of between 2 and 4 were observed. In analogous experiments, replacement of F_H by F_D produced no observable changes in the voltammetry.

(2) Voltammetric Observation of Solvent Isotope Effects. The solvent isotope effects are revealed by exploiting the ability to switch solvent "instantaneously" by transferring the enzyme-coated electrode between solutions. Figure 3 depicts the alternation in catalytic currents observed immediately upon moving between D₂O and H₂O solutions both containing S_H and F_H. For each voltammogram, values of $i_{\text{lim}}^{\text{S}}$, $i_{\text{peak}}^{\text{F}}$, and $i_{\text{lim}}^{\text{F}}$ were measured using the current at the isosbestic potential, $\mathcal{E}_{\text{F/S}}$ (defined separately in H₂O and D₂O, and measured during the experiment) as the zero level. Each time the enzyme is moved from D₂O into H₂O there is an immediate increase in current; conversely when moving from H₂O to D₂O the corresponding decrease in current is observed. There is obviously also an

(14) Glasoe, P. K.; Long, F. A. *J. Phys. Chem.* **1960**, *64*, 188–190.

(15) Subscripts refer to complete deuteration (D) or protonation (H) of C₂ and C₃.

(16) Williamson, J. R.; Corkey, B. E. *Methods Enzymol.* **1969**, *13*, 463–466.

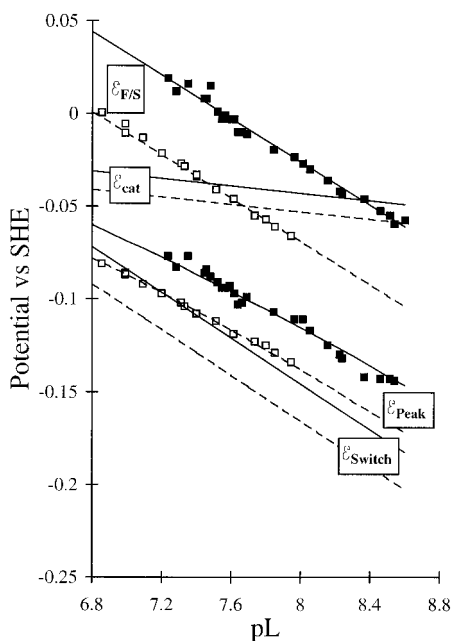


Figure 4. The potential-domain characteristics of succinate dehydrogenase. Variation of potential parameters with pL for the thermodynamically defined all-H and all-D systems. The graph shows observed parameters $\mathcal{E}_{F/S}$ and \mathcal{E}_{peak} as points, and indicates respective lines for the computed parameters \mathcal{E}_{cat} , \mathcal{E}_{switch} , and \mathcal{E}_{peak} (modeled). Key: L = D (— and ■) and L = H (- - and □). Note that the point where $\mathcal{E}_{F/S}$ and \mathcal{E}_{cat} cross is the pL at which the enzyme system is energetically unbiased in its direction of catalysis.

overall decrease in activity over time as the enzyme activity decays. Values for the current ratios (H_2O/D_2O) were obtained by fitting the decay in activity to an exponential function. Similar results were obtained whether the experiment commenced in D_2O or H_2O , while the ratios of activity were virtually constant for the duration of the entire experiment, showing that the catalytic energetics are not influenced by slower secondary H/D substitutions at ionizable residues in the enzyme. The ratios of rates (currents measured in H_2O normalized with respect to those in D_2O) are shown in Figure 3 for pL = 7.4 ($i_{lim}^S = 2.5 \pm 0.4$, $i_{peak}^F = 3.1 \pm 0.4$, and $i_{lim}^F = 2.1 \pm 0.4$); those for pL = 7.8 are similar ($i_{lim}^S = 2.15 \pm 0.25$, $i_{peak}^F = 2.80 \pm 0.25$, and $i_{lim}^F = 2.15 \pm 0.25$).^{17,18}

(3) Overall Isotope Effects: Substitution of Both Solvent and Substrate and a Description of Energetics in the Potential Domain. To this point, we have addressed as separate entities the isotope effects due to organic substrate and solvent. In summary, there is a decrease in the rate on deuterating succinate but not fumarate (as expected from conventional experiments), and a decrease in both rates of catalysis on deuterating solvent—although the influence on fumarate reduction is somewhat greater. The immediate suggestion is that, as anticipated, proton-transfer processes are a major factor limiting rates of catalytic electron transport in SDH. Considering the reaction taking place (eq 1), we might expect that the nature of the “in-flight” L nucleus would determine the rate of the L-transfer reaction—and consequently that the major effects

(17) The same procedure was used to attempt a proton inventory—experiments to determine the solvent isotope effect were carried out in varying mole fractions of D_2O/H_2O . A linear relationship is expected for the involvement of a single exchangeable proton, a quadratic relationship for two protons etc. (Klinman, J. P. *Adv. Enzymol. Relat. Areas Mol. Biol.* **1978**, *46*, 415–494; see also ref 10). The results obtained indicated the possibility of using the voltammetric technique in such a way; however, although the data showed an approximately linear trend the errors were sufficiently significant that curvature could not be excluded.

(18) We also noted greater separation between isosbestic potentials measured for oxidative and reductive scans in D_2O compared to H_2O . The basis for this hysteresis is under investigation.

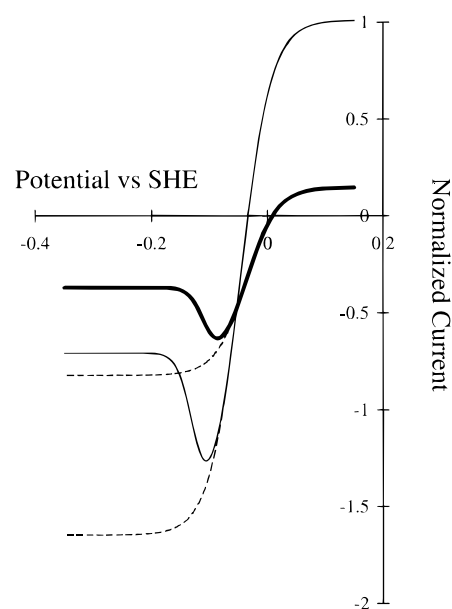


Figure 5. Modeled voltammograms for all-H (faint line) and all-D (bold line) systems at equal pL (7.4), showing the consensus effects on characteristic potentials and currents. Broken lines indicate the voltammetry predicted in the absence of a switch (note also that the observed magnitude of the fumarate reduction isotope effect is influenced by the relative positions of \mathcal{E}_{cat} and \mathcal{E}_{switch}).

should occur upon deuterating succinate (oxidation) and deuterating solvent (reduction). However, this is not a completely satisfactory explanation since changes in the energetics of the system have not been taken into account. Protein film voltammetry enables changes in rate (current) to be viewed alongside alterations in substrate and enzyme potentials; thus by utilizing the voltammetric markers, the relative bidirectional kinetics can be described in the *potential* (driving force) domain rather than the *current* (kinetic) domain. We therefore compared the *thermodynamically definable* all-H and all-D systems. (A Nernstian equilibrium can be established for F_H/S_H in H_2O and F_D/S_D in D_2O , but not, for example, for F_D/S_D in H_2O , F_D being converted to the undefined “ S_{DH} ”).

Voltammetry carried out as before, by exchanging an electroactive enzyme film between $F_H/S_H/H_2O$ and $F_D/S_D/D_2O$, gave ratios in currents which were consistent with a compounding of substrate and solvent effects. For i_{lim}^S even greater amplitude oscillations were now observed than for S_H vs S_D measured in H_2O , while values for i_{peak}^F and i_{lim}^F were similar to those observed for solvent effects alone.¹⁹ In Figure 4 the experimental parameters $\mathcal{E}_{F/S}$ and \mathcal{E}_{peak} are plotted against pL, and values of \mathcal{E}_{switch} and \mathcal{E}_{cat} estimated using our model⁶ are also shown. To illuminate the emerging picture, Figure 5 shows consensus voltammograms displaying the changes in characteristic potentials and relative currents for the all-H and all-D-substituted systems. Values of the substrate reduction potential $\mathcal{E}_{F/S}$ for the all-D system run parallel to those for the all-H system (gradient = $\ln 10 RT/2F$)²⁰ but are increased by 43 mV, showing that succinate is stabilized with respect to fumarate. The corresponding change in equilibrium constant (K_L) for exchange of L between organic substrate and solvent (F_L and L^+_{aq} in equilibrium with S_L and L_2O) as given by K_D/K_H is 25. The result reflects many different factors such as C—H/D bond strength, pK, solvation, and H-/D-bonding and is consistent with

(19) Overall H/D current ratios are as follows: i_{lim}^S , 6.5 ± 0.50 (pL 7.4) and 5.6 ± 0.50 (pL 7.8); i_{peak}^F , 2.60 ± 0.50 (pL 7.4) and 2.20 ± 0.50 (pL 7.8); and i_{lim}^F , 2.00 ± 0.50 (pL 7.4) and 1.90 ± 0.50 (pL 7.8).

measurements made on other systems. In particular we note²¹ that the potential of the quinhydrone electrode (used extensively for measuring the changes in pK of weak acids²²) changes by 34.5 mV on deuteration. Further examples are given in ref 23. To confirm the reliability of this result we measured the purity of succinate and fumarate samples using both C, H, O elemental analysis and enzymatic redox assay as described in the experimental section. The results for S_H, S_D, and F_H gave purity values of 98–102%, while values obtained for F_D gave 96–100%. For the greatest possible error in the 1:1 succinate:fumarate ratio the Nernst equation indicates a difference of less than 1 mV between true and measured values of $\bar{E}_{F/S}$. Errors in measuring $\bar{E}_{F/S}$ were estimated to be ± 2 mV.

Similarly, there is a small increase (~ 20 mV) in E_{peak} , which on the basis of our model translates to an increase in E_{switch} and thus stabilization of reduced FAD. The effect is similar to the increase in the reduction potential observed upon deuteration of the FAD in xanthine oxidase, as reported by Hille.¹¹ Indeed, under no conditions are the H- and D-media voltammograms superimposable; thus the fact that at least one of the values $\bar{E}_{F/S}$ and E_{switch} must shift by at least 20 mV in order to produce the greater separation is unavoidable. The relatively small increase of 10 mV in E_{cat} is consistent with this parameter being a convolution of all electron-transfer centers in the enzyme (not only the FAD). For example, Fe–S centers tend to show only a mild variation of potential with pH^{1a}.

We now consider the effects which these shifts in potential exert upon the activity of the enzyme. First, and independently of any constant offset²⁴ which is produced in all the potentials, it is the *difference* between the intrinsic potential characteristics of the enzyme (E_{cat} , E_{switch}) and $\bar{E}_{F/S}$ which determines the catalytic activity. In particular, upon deuteration, a significant shift in the catalytic bias ($E_{\text{cat}} - \bar{E}_{F/S}$) is produced and the pL for equal bias (at which $E_{\text{cat}} = \bar{E}_{F/S}$) is raised from 7.65 to 8.35 (see Figure 4). In terms of energetics, this confirms the observation that SDH in D-media is even more biased toward fumarate reduction. (The fumarate isotope effect is less than the succinate isotope effect.¹⁹) The solvent isotope effect data are now more clearly explained. Attenuation of the succinate oxidation rate upon changing to D₂O is (at least partly) accountable for by less favorable ET energetics. On the other hand, fumarate reduction is attenuated despite the *more* favorable ET energetics (electron transfer from the enzyme (E_{cat}) to fumarate ($\bar{E}_{F/S}$) is thermodynamically more favored), thus showing that the rate of transfer of protons^{8,9} derived from solvent imposes an intrinsic kinetic barrier to electron transport. Most likely this will reflect transfer of H(D) between the flavin and fumarate, the reverse of the substrate isotope effect observed with succinate. Observation of a significant isotope effect on fumarate reduction for the less-active low-potential form of the enzyme also indicates that the difference in activity between the two forms does not reside in H-transfer limitations.

In conclusion, these experiments reveal an alternative perspective on isotope effects in enzymatic electron transport and

suggest both the importance and possibilities of gaining a “global” picture of proton-transfer energetics in (and particularly for) the most complex systems. Traditionally used kinetic parameters (observed rates) are now separated from the contributions of catalytic bias (energetics), and the compounded effects of H/D substitution are thereby related naturally to both thermodynamic requirements and kinetic limitations.

Acknowledgment. This work was funded by The Wellcome Trust (grant no. 042109), The Royal Society, the UK EPSRC (Quota award, J. H.) and the US National Institutes of Health (USPHS program HL-16251). J.H. and F.A.A. thank Theakstons XB and the Lamb and Flag for valuable help.

Appendix 1: Modeling of the Catalytic Waveform

To explain the voltammetric waveform observed for catalysis by adsorbed SDH, we consider first the simplest case of a reversible redox couple, the oxidized and reduced forms of which are at equal concentration in solution. The electrode reaction is uncatalyzed and mass transport controlled. The resulting sigmoidal potential–current response is shown in Figure A1. At both high and low potentials, the current reaches limiting values i_{lim} which are in a ratio 1:1 if oxidant (e.g., fumarate, F) and reductant (e.g., succinate, S) have similar diffusion coefficients. In the intermediate potential region is a simple Nernstian curve intersecting the potential (zero-current) axis at the formal reduction (half-wave) potential and with a steepness defined by n , the number of electrons transferred in the electrode process. We show here the curve expected for an $n = 2$ reaction, no stable radical being involved.

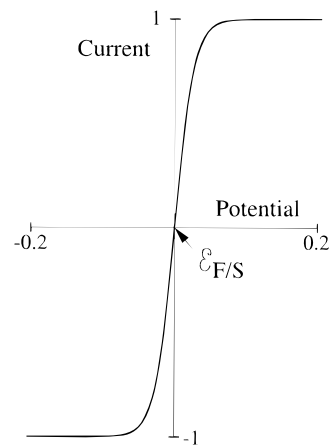


Figure A1.

We now extend this description to a redox couple which is *inactive* at the electrode, but becomes active if the electrode is modified with a catalyst, i.e., an adsorbed enzyme with redox-active centers. Figure A2 depicts the voltammogram for a 1:1 mixture of F and S, in the (special) case where the effective reduction potential of the enzyme E_{cat} matches that of the solution redox couple, $\bar{E}_{F/S}$. The electrode reaction is no longer mass transport controlled; instead the limiting currents in either direction are controlled by the enzyme, as is the n value. The ratio of limiting currents $i_{\text{lim}}^{\text{S}}$ and $i_{\text{lim}}^{\text{F}}$ is 1.0 because $E_{\text{cat}} = \bar{E}_{F/S}$ and the enzyme has no bias toward catalysis in either direction. The n value corresponds to the number of electrons in the rate-determining enzyme step (in this case one) rather than two as observed for the uncatalyzed reaction. The enzyme, unlike substrate alone, has the capability to process one-electron states.

Next we consider the case where $E_{\text{cat}} \neq \bar{E}_{F/S}$, and the enzyme thus possesses a catalytic bias. Figure A3 shows the voltammetry expected for the situation $E_{\text{cat}} < \bar{E}_{F/S}$ where the enzyme's

(20) Values of $\bar{E}_{F/S}$ and E_{peak} measured for the 100% H system are 18 mV more negative than reported recently in ref 6. This figure lies outside of experimental error and at present we have no satisfactory explanation. The conclusions of these experiments, which directly compare H/D effects in the same system, are not affected.

(21) La Mer, V. K.; Korman, S. *J. Am. Chem. Soc.* **1935**, *57*, 1511.

(22) McDougall, A. O.; Long, F. A. *J. Phys. Chem.* **1962**, *66*, 429–433.

(23) La Mer, V. K.; Korman, S. *Science* **1936**, *83*, 624–626. La Mer, V. K. *Chem. Rev.* **1936**, *19*, 363–374.

(24) It is possible that an extra Junction Potential exists between the D₂O solutions used and the Standard Calomel Electrode (saturated KCl in H₂O). We would however expect this to be a relatively small contribution (<5 mV); see: La Mer, V. K.; Noonan, E. *J. Am. Chem. Soc.* **1939**, *61*, 1487–1491. Salomaa, P. *Acta Chem. Scand.* **1971**, *25*, 365–366.

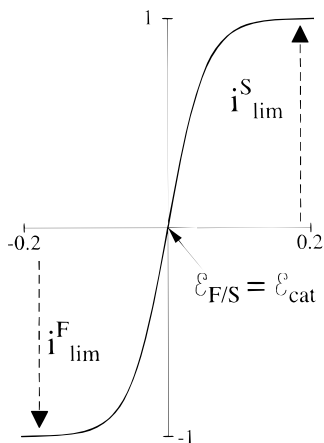


Figure A2.

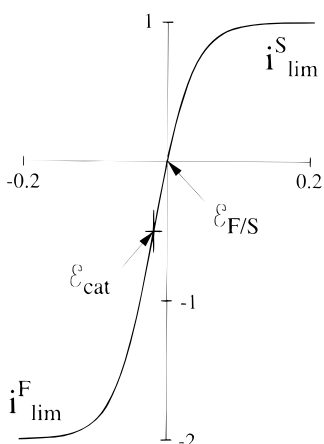


Figure A3.

redox centers are better tuned to catalyze in the reductive direction. The voltammogram has the same shape as given in Figure A2 (the n value is still one) but is displaced. The curve intersects the potential axis at $E_{F/S}$ as required, but now $i_{lim}^F > i_{lim}^S$. Obviously at i_{lim}^F and i_{lim}^S , interfacial electron transfer is not rate limiting and as above, the catalytic rate is determined by factors intrinsic to the enzyme. For bidirectional catalysis, the ratio of limiting currents equates to the ratio of rate (specificity) constants as given by the Haldane equation, i.e., $i_{lim}^S/i_{lim}^F = (k_{cat}^{SF}K_M^F)/(k_{cat}^{FS}K_M^S)$.²⁵

Referring back to Figure 1, we note that the fumarate reduction current does not follow the broken line to the bottom of the sigmoidal wave (broken line) but instead decreases quite sharply below a potential E_{peak} (maximum current i_{peak}^F) and settles at a lower value of i_{lim}^F . This interesting effect, that of a reaction rate decreasing as the driving force is increased resembles a “tunnel diode”, a device that displays *negative* resistance in a certain region of potential bias. It is possible to reproduce this behavior exactly by including a second Nernstian redox couple, reduction potential E_{switch} , assigned to two-electron reduction of the FAD, which converts the enzyme to a less active form E_{red}^* . This interconversion is represented at the center of Scheme 1, with less active (asterisk) and more stable (underlined) states indicated. Scheme 1 comprises two adjoining catalytic cycles differing in values of rate and equilibrium parameters: the cycle at the right-hand side is relevant at potentials more positive than E_{switch} , while the other (having different kinetic constants) is relevant when the FAD prevails in the reduced conformation. The lower value of i_{lim}^F is not relevant to the ratio of specificity constants described above, which pertain only to the more active form.

(25) *Enzyme Structure and Mechanism*; Fersht, A.; W. H. Freeman and Co.: New York, 1985.

Appendix 2: The Catalytic Bias of an Enzyme

Each step in Scheme 1 is defined by a measurable equilibrium or a ratio of rate constants. Shown vertically at the center of the diagram is the interconversion between free fumarate and succinate, with reduction potential $E_{F/S}$. This otherwise irreversible electrode reaction is catalyzed by adsorbed SDH in a series of steps represented as cycles to either side. We consider only the more active form of the enzyme (right-hand side) and note that consecutive equilibria connect S back to F. Proceeding counterclockwise, we identify binding of succinate to oxidized enzyme E_{ox} (defined by $1/K_D^S$), intramolecular exchange of two electrons within the enzyme–substrate complex ($k_{cat}^{SF}/k_{cat}^{FS}$), transfer of electrons between the enzyme–substrate complex and the electrode (represented by E_{cat}) and release of fumarate from the enzyme (K_D^F). At equilibrium, the cycle is stationary and the free-energy terms sum together as

$$2F(E_{F/S} - E_{cat}) + RT \ln \left(\frac{K_D^F}{K_D^S} \right) - RT \ln \left(\frac{k_{cat}^{FS}}{k_{cat}^{SF}} \right) = 0 \quad (A1)$$

To define thermodynamically the catalytic bias we take into account that $n = 2$ as required in the cycle, but $n = 1$ when measured from the wave shape. By considering simple Nernstian wave shapes for both succinate oxidation and fumarate reduction we write

$$i_s = \frac{i_{lim}^S}{1 + \exp [(nF)/(RT)(E_{1/2} - E)]} \quad (A2)$$

$$|i_F| = \frac{|i_{lim}^F|}{1 + \exp [(nF)/(RT)(E - E_{1/2})]}$$

We identify E_{cat} with $E_{1/2}$, the half-wave potential and $E_{F/S}$ with the potential at which $i_s = |i_F|$. Equating the two above expressions gives, at $E_{F/S}$

$$(nF)(RT)(E_{F/S} - E_{cat}) = \ln[|i_{lim}^F|/i_{lim}^S] \quad (A3)$$

The term $(E_{F/S} - E_{cat})$ can now be used to quantify the catalytic bias after adjustment to accommodate $n = 2$ as required by the thermodynamic cycle and $n = 1$ as measured from the wave shape:

$$(E_{F/S} - E_{cat})_{cycle} = (n_{meas}/n_{cycle})(E_{F/S} - E_{cat})_{meas} \quad (A4)$$

Substituting into eq A1 we obtain

$$(E_{cat} - E_{F/S})_{meas} = \frac{RT}{2F} \frac{n_{cycle}}{n_{meas}} \ln \left(\frac{k_{cat}^{SF}K_D^F}{k_{cat}^{FS}K_D^S} \right) \quad (A5)$$

which relates the catalytic bias (for $K_D \approx K_M$ this is the ratio of specificity constants in each direction) to the difference between the effective reduction potential of the enzyme and that of the redox reaction being catalyzed.